

R-branch high-lying transition emission spectra of SbNa molecule

Chun-Run Luo(罗春润), Qun-Chao Fan(樊群超), Zhi-Xiang Fan(范志祥), Jia Fu(付佳)\ccclink, Jie Ma(马杰), Hui-Dong Li(李会东), and Yong-Gen Xu(徐勇根)

Citation: Chin. Phys. B, 2021, 30 (**1**): 013301. DOI: 10.1088/1674-1056/abc3b2
Journal homepage: http://cpb.iphy.ac.cn; http://iopscience.iop.org/cpb

What follows is a list of articles you may be interested in

Study on the $A^2\Pi_{3/2u}$, $B^2\Delta_{3/2u}$, and $X^2\Pi_{3/2g}$ states of Cl_2^+ including its isotopologues

Wu Ling, You Su-Ping, Shao Xu-Ping, Chen Gang-Jin, Ding Ning, Wang You-Mei, Yang Xiao-Hua
Chin. Phys. B, 2015, 24 (**8**): 083301. DOI: 10.1088/1674-1056/24/8/083301

Assignment of terahertz vibrational modes of L-glutamine using density functional theory within generalized-gradient approximation

Zhang Han, Zhang Zhao-Hui, Zhao Xiao-Yan, Zhang Tian-Yao, Yan Fang, Shen Jiang
Chin. Phys. B, 2015, 24 (**7**): 073301. DOI: 10.1088/1674-1056/24/7/073301

High-resolution photoassociation spectroscopy of ultracold Cs_2 long-range 0_g^- state： The external well potential depth

Liu Wen-Liang, Wu Ji-Zhou, Ma Jie, Xiao Lian-Tuan, Jia Suo-Tang
Chin. Phys. B, 2014, 23 (**1**): 013301. DOI: 10.1088/1674-1056/23/1/013301

High resolution photoassociation spectra of an ultracold Cs_2 long-range 0_u^+ ($6S_{1/2}$+$6P_{1/2}$) state

Chen Peng, Li Yu-Qing, Zhang Yi-Chi, Wu Ji-Zhou, Ma Jie, Xiao Lian-Tuan, Jia Suo-Tang
Chin. Phys. B, 2013, 22 (**9**): 093301. DOI: 10.1088/1674-1056/22/9/093301

Low-frequency vibrational modes of glutamine

Wang Wei-Ning, Wang Guo, Zhang Yan
Chin. Phys. B, 2011, 20 (**12**): 123301. DOI: 10.1088/1674-1056/20/12/123301

R-branch high-lying transition emission spectra of SbNa molecule*

Chun-Run Luo(罗春润)[1], Qun-Chao Fan(樊群超)[1,†], Zhi-Xiang Fan(范志祥)[1,‡], Jia Fu(付佳)[1,§], Jie Ma(马杰)[2], Hui-Dong Li(李会东)[1], and Yong-Gen Xu(徐勇根)[1]

[1] *School of Science, Research Center for Advanced Computation, Xihua University, Chengdu* 610039, *China*
[2] *State Key Laboratory of Quantum Optics and Quantum Optics Devices, Laser Spectroscopy Laboratory, College of Physics and Electronics Engineering, Shanxi University, Taiyuan* 030006, *China*

(Received 12 September 2020; revised manuscript received 21 October 2020; accepted manuscript online 22 October 2020)

The calculation results of the *R*-branch transition emission spectra of (0–0) band of the $A_2 1 \rightarrow X_2 1$ transition system of SbNa molecule are presented in this paper. These *R*-branch high-lying transitional emission spectral lines are predicted by using the difference converging method (DCM). Our results show excellent agreement between DCM spectral lines and the experimental values, and the deviations are controlled within 0.0224 cm^{-1}. What is more, based on the principle of over-determined linear equations, the prediction error is quantified in this work, which provides reliable theoretical support for our predicted DCM calculations. This work provides a lot of useful information for understanding the microstructure of SbNa molecule.

Keywords: SbNa, transitional spectral lines, *R*-branch, difference converging method

PACS: 31.13.–P, 33.20.Vq **DOI:** 10.1088/1674-1056/abc3b2

1. Introduction

The antimonide is one of the most abundant elements of the mineral resources in the world.[1] Antimony compounds play a significant role in the chemical industry and electronic industry.[2–5] For instance, the antimony–sodium (SbNa) not only has a lowcost and simple preparation process, but also possesses a short response time and high sensitivity in the visible and near-infrared range, thus becoming one of the concerned photocathode materials.[6,7] However, uncertainties of the exact structure and physical mechanism bring the difficulty into theoretical guidance of manufacturing technique, which leads to over reliance on past experience in the production, thereby limiting the improvement of its performance.[8] In order to optimize the production and processing technology of SbNa-related materials, we need to explore the microcharacteristics of SbNa molecule by obtaining more exact rovibrational transition lines, which are valuable in understanding basic molecular structure.[9–11]

Long-term since, many research groups have focused on SbNa. In 1971, Evans and Watson[12] presented a new method of melting the antimony in sodium at 190 °C–550 °C. This method should be also suitable for studying the solubility of mixed solutes. In 1982, Redslob *et al.* reported a part of the new measurements of thermoelectric power, electrical conductivity, magnetic susceptibility and molar volume of liquid Na–Sb alloy. According to its electronic characteristics, it is confirmed that there is a typical semiconductor behavior within a certain range.[13] In 1985, Dolizy and Groliere used optical transmittance and Auger electron spectroscopy (AES) analyses to obtain some alkali antimonide compounds' thermodynamic data, deduced and discussed the dissociation behavior of alkali antimonide varying with temperature and time.[14] In 1993, Songster and Pelton reported the phase diagram, thermochemical properties and phase equilibrium data of the Sb–Na binary system.[15] In 2013, Liu *et al.* modeled the Sb–Na binary system to facilitate the calculation and design of new fusible alloys based on experimental data, and reproduced the relevant thermochemical properties and phase diagram characteristics as well.[16] What is more, Setzer *et al.* were interested specially in the group Va-alkali, they reported transition emission spectral lines of all seven transitions from five low-lying excited states data of SbNa in 2015.[17] Phoebek *et al.* demonstrated the separation of amorphous and crystalline phases formed in a sodium-ion battery for the first time by tracking Sb–Na phase transformations in sodium-ion anodes.[18] However, there is still lack of research on direct correctly high-lying excitation rotational quantum states data of SbNa, because of the limitations of current experimental equipment.

About theoretic calculation for transition spectra, the first principle calculation is a common calculation method used in the low-lying electronic states of antimony-containing diatomic molecules.[19,20] Due to the mutual interference of

*Project supported by the Sichuan Education Department Project, China (Grant No. 17ZA0369), the Fund for Sichuan Distinguished Scientists of China (Grant Nos. 2019JDJQ0050 and 2019JDJQ0051), the National Natural Science Foundation of China (Grant Nos. 61722507 and 11904295), and the State Key Laboratory Open Fund of Quantum Optics and Quantum Optics Devices, Laser Spectroscopy Laboratory, China (Grant Nos. KF201811 and KF2020003).

†Corresponding author. E-mail: fanqunchao@sina.com
‡Corresponding author. E-mail: fanzhixiang235@126.com
§Corresponding author. E-mail: fujiayouxiang@126.com

© 2021 Chinese Physical Society and IOP Publishing Ltd

various coupling effects in the system, the theoretical prediction of high-lying excited rotational quantum states needs a large amount of calculation.[21] For a certain diatomic molecule, the calculation error of dissociation energy may be at a 10^2 cm^{-1} level, while vibration energy error may be at 10 cm^{-1} level.[20,22]

More recently, the difference converging method (DCM) suggested by Fan *et al.* was used to calculate radiative opacities for hot metal plasmas,[23] differential cross sections (DCSs) of electron scattering from polyatomic molecules,[24] and transition spectral lines for diatomic molecules.[9,25,26] Among these cases, good predictions can be achieved by using the DCM treatment. In an effort to further understand the theoretical errors and accuracy for transition spectral lines, in the present paper we use the DCM and the principle of over determined linear equations to study the R-branch high-lying transition emission spectral lines of (0–0) band of the $A_2 1 \rightarrow X_2 1$ transition of SbNa molecule. And, considering the source and propagation of the prediction error, the principle of over determined linear equations can be applied to interpolation and extrapolation, which yields an average prediction error at a 10^{-2} cm^{-1} level.

2. Theory and method

The classical expression of the R-branch transition spectral lines can be expressed as[27]

$$\begin{aligned} \nu \;=\; & \nu_0 + (J+1)\left[B_{\upsilon'}(J+2) - B_{\upsilon''}J\right] \\ & - (J+1)^2\left[D_{\upsilon'}(J+2)^2 - D_{\upsilon''}J^2\right] \\ & + (J+1)^3\left[H_{\upsilon'}(J+2)^3 - H_{\upsilon''}J^3\right] \\ & + (J+1)^4\left[L_{\upsilon'}(J+2)^4 - L_{\upsilon''}J^4\right] + \cdots, \end{aligned} \tag{1}$$

where J and υ are the rotational quantum number and vibrational quantum number, $\{L_{\upsilon'}, L_{\upsilon''}, H_{\upsilon'}, H_{\upsilon''}, D_{\upsilon'}, D_{\upsilon''}, B_{\upsilon'}, B_{\upsilon''}\}$ are the rotation spectral constants. ν is the energy difference of rotational transition. ν_0, the sum of the electronic state energy and the vibration energy, is a constant for the vibration transition.

Equation (1) can be applied to all transition states of the same transition band. Combining the idea of difference, we can further transform it into a functional form of the spectral constant $L_{\upsilon(1\sim4)''}$ through the quadratic difference of $\nu_1 - \nu_2$ and $\nu_3 - \nu_4$. Similarly, it is easy to transform into a functional form of the spectral constant $L_{\upsilon(2\sim5)''}$ through the second-order difference of $\nu_2 - \nu_3$ and $\nu_4 - \nu_5$. Since $L_{\upsilon(1\sim4)''} = L_{\upsilon(2\sim5)''}$, the $L_{\upsilon''}$ can be eliminated by further simplification, and the expression of $L_{\upsilon(1\sim5)'}$ can be obtained similarly, the derivation process is also fit for $L_{\upsilon(2\sim6)'}$. Then, we can simplify and obtain the rotation spectral constant $L_{\upsilon'}$. In this way, the rotation spectral constants $\{L_{\upsilon'}, L_{\upsilon''}, H_{\upsilon'}, H_{\upsilon''}, D_{\upsilon'}, D_{\upsilon''}, B_{\upsilon'}, B_{\upsilon''}\}$ in Eq. (1) can be expressed by the expression composed of transition lines $\nu_1 \sim \nu_{12}$ and the corresponding rotational quantum number $J_1 \sim J_{12}$. With the idea of the difference, a new analytical formula without any spectral constant can be finally simplified and sorted as follows:[9]

$$\begin{aligned} \nu_{J_{12}} \;=\; & \nu_{J_1}C_1 + \nu_{J_2}C_2 + \nu_{J_3}C_3 + \nu_{J_4}C_4 + \nu_{J_5}C_5 + \nu_{J_6}C_6 \\ & + \nu_{J_7}C_7 + \nu_{J_8}C_8 + \nu_{J_9}C_9 + \nu_{J_{10}}C_{10} + \nu_{J_{11}}C_{11}, \end{aligned} \tag{2}$$

where $\nu_{J_1} \sim \nu_{J_{11}}$ are the 11 best selected experimental data, $C_1 \sim C_{11}$ are the expansion coefficients which are directly related to the rotation quantum numbers $J_1 \sim J_{12}$. It is worth mentioning that as long as the expansion coefficients and 11 experimental transition lines are ensured we can accurately predict the transition spectra of R-branch system.

For a certain transition band of a given diatomic molecule, we can select 11 transition lines from the m known experimental spectral lines, then there are $N = C_m^{11}$ choices. There is a set of physical criteria to make us clearly to find out the best data.

$$\left|\nu_{J,\mathrm{expt}} - \nu_{J,\mathrm{cal}}\right| \rightarrow 0, \tag{3}$$

$$\left|\Delta_{J,\mathrm{expt}} - \Delta_{J,\mathrm{cal}}\right| \rightarrow 0, \quad \Delta_J = \nu_{J-1} - \nu_J, \tag{4}$$

$$\left|\Delta_{J,\mathrm{expt}}/\nu_{J-1,\mathrm{expt}}\right| - \left|\Delta_{J,\mathrm{cal}}/\nu_{J-1,\mathrm{cal}}\right| \rightarrow 0, \tag{5}$$

where $\left|\nu_{J,\mathrm{expt}} - \nu_{J,\mathrm{cal}}\right|$ denotes the difference between experimental and theoretical values, $\Delta_J = \nu_{J-1} - \nu_J$ is the first spectral difference, $\left|\Delta_{J,\mathrm{expt}} - \Delta_{J,\mathrm{cal}}\right|$ is the difference between the experimental values and the theoretical calculations. "$\rightarrow 0$" ensures that theoretical errors in Eqs. (3)–(5) should be as small as possible. And equation (3) has the priority to ensure the sufficient spectral accuracy of the calculated transition lines. Then the most suitable for this spectral line is one of the best physical representations of the real lines of the molecular system. Based on the DCM, combined with the finite experimental transition data and the classical expression of the total energy level of molecule, the unknown R-branch transition spectra can be predicted theoretically by multiple difference and physical criterion screening.

There is no doubt that a certain error $\Delta\nu_{J_1}$ between the experimental value and the actual value is inevitable, so equation (2) can be changed into

$$\begin{aligned} \nu'_{J_{12}} \;=\; & (\nu_{J_1} + \Delta\nu_{J_1})C_1 + (\nu_{J_2} + \Delta\nu_{J_2})C_2 + (\nu_{J_3} + \Delta\nu_{J_3})C_3 \\ & + (\nu_{J_4} + \Delta\nu_{J_4})C_4 + (\nu_{J_5} + \Delta\nu_{J_5})C_5 \\ & + (\nu_{J_6} + \Delta\nu_{J_6})C_6 + (\nu_{J_7} + \Delta\nu_{J_7})C_7 \\ & + (\nu_{J_8} + \Delta\nu_{J_8})C_8 + (\nu_{J_9} + \Delta\nu_{J_9})C_9 \\ & + (\nu_{J_{10}} + \Delta\nu_{J_{10}})C_{10} + (\nu_{J_{11}} + \Delta\nu_{J_{11}})C_{11}, \end{aligned} \tag{6}$$

where $\Delta\nu_{J_i}$ $(i = 1, 2, \ldots, 11)$ are the errors introduced in experiment. By comparing Eq. (2) with Eq. (6), the prediction error

caused by experimental uncertainty is

$$\Delta\delta = C_1\Delta\nu_{J_1} + C_2\Delta\nu_{J_2} + C_3\Delta\nu_{J_3} + C_4\Delta\nu_{J_4} + C_5\Delta\nu_{J_5} + C_6\Delta\nu_{J_6} + C_7\Delta\nu_{J_7} + C_8\Delta\nu_{J_8} + C_9\Delta\nu_{J_9} + C_{10}\Delta\nu_{J_{10}} + C_{11}\Delta\nu_{J_{11}}. \quad (7)$$

It is worth noticing that all high-lying transitional emission spectral lines can be predicted by Eq. (2). Supposing that the main reason for the theoretical error is the experimental uncertainty of the selected 11 transition lines, and can be estimated from Eq. (7). So, if there are m (> 11) known experimental transition lines, there will be m linear equations

$$\begin{aligned}\Delta\delta_J &= \nu_J^{\rm cal} - \nu_J^{\rm exp} \\ &= C_1(J)\Delta\nu_{J_1} + C_2(J)\Delta\nu_{J_2} + C_3(J)\Delta\nu_{J_3} + C_4(J)\Delta\nu_{J_4} \\ &\quad + C_5(J)\Delta\nu_{J_5} + C_6(J)\Delta\nu_{J_6} + C_7(J)\Delta\nu_{J_7} + C_8(J)\Delta\nu_{J_8} \\ &\quad + C_9(J)\Delta\nu_{J_9} + C_{10}(J)\Delta\nu_{J_{10}} + C_{11}(J)\Delta\nu_{J_{11}}. \end{aligned} \quad (8)$$

There are 11 independent variables $(\Delta\nu_{J_1\sim J_{11}})$ and m (> 11) equations in Eq. (8). Based on the principle of over determined linear equations $\Delta\nu_{J_I} = (C_i'C_i)^{-1} \times C_i'\sigma$ $(i = 1,2,\ldots,11)$, where C_i $(i = 1,2,\ldots,11)$ denote the expansion coefficients, C' is the transposing of the C matrix and the σ is the difference between the experimental value and the theoretical one, the error $\Delta\nu_{J_i}$ $(i = 1,2,\ldots,11)$ can be estimated. Once $\Delta\nu_{J_i}$ $(i = 1,2,\ldots,11)$ is determined, we can use Eq. (8) to estimate the error by the unknown experimental data predicted by the formula.

3. Results and discussion

Using the DCM, we calculate the R-branch transition emission spectral lines of (0–0) band of the $A_21 \rightarrow X_21$ transition system of SbNa molecule in this work. The best 11 selected experimental spectral lines are collected in Table 1, where the moderate error $\Delta\nu_{J_i}$ $(i = 1,2,\ldots,11)$ values are effectively estimated from Eq. (8), allowing for a rapid prediction in the R-branch transition calculation. Through the merit of the DCM approach, the numerical values of the R-branch transition emission spectral lines are easily obtained, which are listed in Table A1 and Table A2 (see Appendix A), where the $R_{\rm e}$ branch and $R_{\rm f}$ branch emission spectral lines are given up to $J_{\rm max}^{\rm Cal} = 120$. Additionally, the calculated transition lines are listed with the appropriate number of significant digits corresponding to the experimental ones. As can be seen from Table A1, differences between experimental spectral lines and the DCM data are on average less than ± 0.005 cm^{-1}, and displayed in Fig. 2(a). In addition to the comparison among the transition lines, an illustration for the $R_{\rm e}$ branch of the (0–0) band of the $A_21 \rightarrow X_21$ system is provided in Fig. 1(a), in which the DCM transition spectral lines and experimental ones overlap with each other. Furthermore, in order to confirm the accuracy of the DCM prediction, especially in the high J lines without the comparison of the possible measurement with the theoretical transition lines, it is worthwhile to emphasize two important theoretical aspects. On the one hand, the estimated error for the theoretical lines should be taken into consideration. Here, with the help of Eq. (8) and the error $\Delta\nu_{J_k}$ values listed in Table 1, the magnitudes of deviation $\Delta\delta$ determined are provided in the last column of Table A1 to access the quality of the DCM prediction determined for $R_{\rm e}$ branch of the (0–0) band. As expected, the magnitudes of deviation $\Delta\delta$ from the DCM values are in agreement satisfactorily with their corresponding line differences listed in the 4th column (also see Fig. 5(a)). As shown in the table, the magnitudes for the deviation $\Delta\delta$ are relatively small in a region of -0.0390 cm^{-1}–0.0027 cm^{-1}, with a spectral resolution of 0.2 cm^{-1}, which indicates that the theoretical DCM lines may be considered to be quite acceptable. On the other hand, assuming the prediction of DCM to be true, the evaluated values for the transition line difference $\Delta_J^{\rm DCM} = \left|\nu_{J-1}^{\rm DCM} - \nu_J^{\rm DCM}\right|$ should be consistent with those from experiment, and can reproduce correctly main experimental trends. As shown in Table A1, the theoretical values of $\Delta_J^{\rm DCM} = \left|\nu_{J-1}^{\rm DCM} - \nu_J^{\rm DCM}\right|$ are found to be in good agreement with the experimental values.

Table 1. Values of rotational quantum number J_k and the error $\Delta\nu_{J_k}$ respectively corresponding to 11 selected known experimental transition lines of (0–0) band of $A_21 \rightarrow X_21$ transition of SbNa molecule.

$R_{\rm e}(J)$ (0,0) band				$R_{\rm f}(J)$ (0,0) band			
J_1	22	$\Delta\nu_{J_1}$	–0.1375	J_1	22	$\Delta\nu_{J_1}$	–0.0349
J_2	27	$\Delta\nu_{J_2}$	–0.3262	J_2	27	$\Delta\nu_{J_2}$	–0.0304
J_3	36	$\Delta\nu_{J_3}$	–0.0725	J_3	28	$\Delta\nu_{J_3}$	–0.0248
J_4	40	$\Delta\nu_{J_4}$	–0.2606	J_4	40	$\Delta\nu_{J_4}$	–0.0259
J_5	44	$\Delta\nu_{J_5}$	–0.0081	J_5	46	$\Delta\nu_{J_5}$	–0.0174
J_6	55	$\Delta\nu_{J_6}$	–0.1953	J_6	65	$\Delta\nu_{J_6}$	–0.0171
J_7	62	$\Delta\nu_{J_7}$	0.0551	J_7	67	$\Delta\nu_{J_7}$	–0.0072
J_8	67	$\Delta\nu_{J_8}$	–0.1297	J_8	70	$\Delta\nu_{J_8}$	–0.0127
J_9	69	$\Delta\nu_{J_9}$	0.1211	J_9	71	$\Delta\nu_{J_9}$	–0.0033
J_{10}	85	$\Delta\nu_{J_{10}}$	–0.0649	J_{10}	75	$\Delta\nu_{J_{10}}$	–0.0025
J_{11}	88	$\Delta\nu_{J_{11}}$	0.1838	J_{11}	78	$\Delta\nu_{J_{11}}$	0.0014

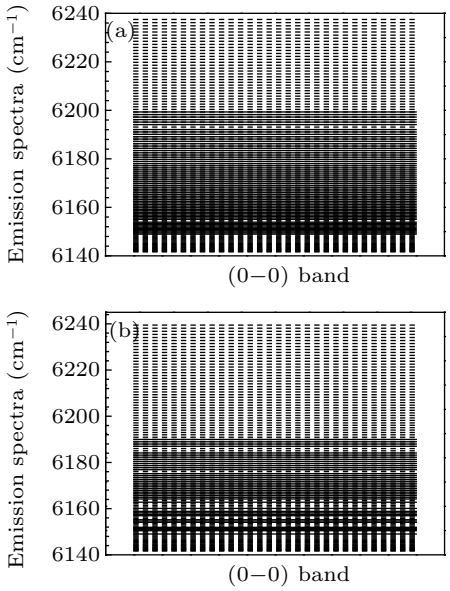


Fig. 1. Experimentally measured (solid line) and theoretically calculated (dashed line) transition lines of R-branch transitional emission spectra of (a) R_e (0–0) band and (b) R_f (0–0) band of $A_2 1 \rightarrow X_2 1$ transition of SbNa.

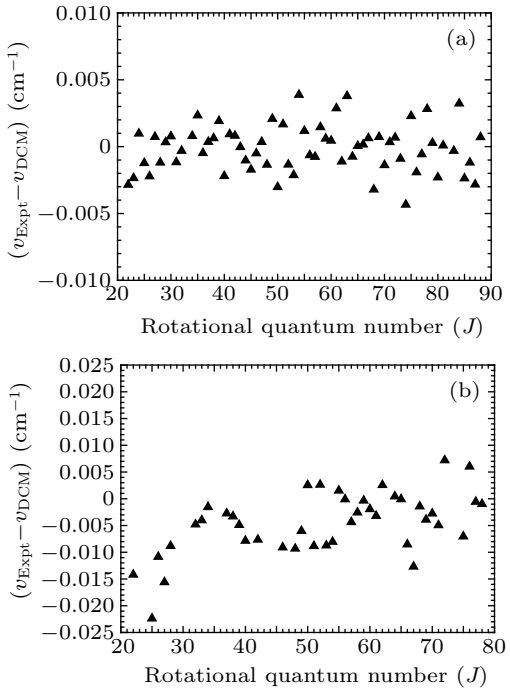


Fig. 2. Difference $(\nu_{J,\mathrm{Expt}} - \nu_{J,\mathrm{Cal}})$ between experimental and theoretical results of (a) R_e (0–0) band and (b) R_f (0–0) band of $A_2 1 \rightarrow X_2 1$ transition of SbNa.

As can be seen from Fig. 3(a), there is a good tendency for theoretical values Δ_J^{DCM} to rise smoothly with the J quantum number increasing from 1 to 120, which is similar to the tendency for the experimental values Δ_J^{Expt}. It is also worth mentioning that the expansion coefficient C varies with the rotational quantum number J as shown in Fig. 4. The expansion coefficient C is a function of J. As indicated in Fig. 4, we can obtain the influence of v_J on spectral line. At about $J = 94$, the R_e branch presents a unique intersection, at this point the calculation error reaches the bottom. It is obvious that $\{C_6, C_8, C_9, C_{10}\}$ change a lot, so the corresponding $\{v_6, v_8, v_9, v_{10}\}$ have a great influence on the prediction of high-lying transitional emission spectral lines. Similarly, at about $J = 82$, the R_f branch presents a unique intersection and $\{C_4, C_5, C_6, C_8, C_9\}$ change greatly, it means that $\{v_4, v_5, v_6, v_8, v_9\}$ have a great influence. There is no doubt that we should pay more attention to the influential wave number for improving experimental accuracy.

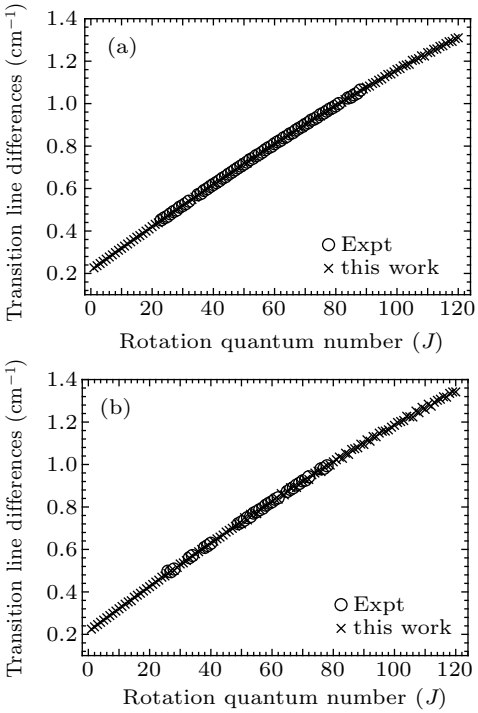


Fig. 3. Experimental and theoretical calculation transition line differences $(\Delta_J = \nu_{J-1} - \nu_J)$ of R-branch transitional emission spectral lines of (a) R_e (0–0) band and (b) R_f (0–0) band of $A_2 0^+ \rightarrow X_1 0^+$ transition of SbNa.

The expected example discussed above allows us to consider another case of the R_f branch emission spectral lines of the (0–0) band of the $A_2 1 \rightarrow X_2 1$ transition system. The values of error $\Delta\nu_{J_k}$ in Table 1 are taken from the spectra analyses described below. As can be seen in Table A2, based on the 72 R_f branch spectral lines reported by Setzer *et al.*,[17] the DCM theoretical spectral lines extracted from Eq. (2) are in fairly good agreement with the available measurements. Another evidence can be found in Fig. 2(b), where differences in $\nu_{J,\mathrm{Expt}} - \nu_{J,\mathrm{DCM}}$ between experimental spectral lines and the DCM data are nevertheless relatively small for most of J-value region with an accuracy of 0.01 cm^{-1}. In Table A2, one can note that, however, the deviation $\Delta\delta$ calculated is slightly larger than that obtained in the first case in the low and high J quantum numbers. Inspection of the deviation $\Delta\delta$ and the difference $\nu_{J,\mathrm{Expt}} - \nu_{J,\mathrm{DCM}}$ between experimental spectral lines and the DCM data reveals that the DCM expansion, namely equation (2), succeeds in reproducing the experimental spectral lines for J-value increasing up to available measurement. This is also graphically confirmed by Fig. 6(a), showing that the deviation $\Delta\delta$ characterized by Eq. (8) accords with the difference value $\nu_{J,\mathrm{Expt}} - \nu_{J,\mathrm{DCM}}$. Again, the extrapolation of the transition line difference $\Delta_J^{\mathrm{DCM}} = \left|\nu_{J-1}^{\mathrm{DCM}} - \nu_J^{\mathrm{DCM}}\right|$ in the low-J and high-J regions yields a similar tendency to what is ob-

tained from the experimental result, which can be found in Fig. 3(b). A contour plot of the expansion coefficient C given in Fig. 4(b) emphasizes that most of the coefficients display small changes in the $J \leq 90$ region, which differs from that obtained in $R_{\rm f}$ branch system.

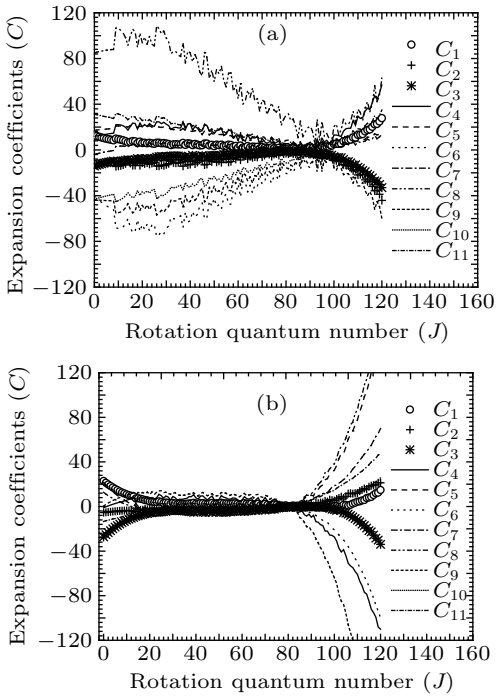


Fig. 4. Variations of expansion coefficients C_i with rotational quantum numbers J of (a) $R_{\rm e}$ (0–0) band and (b) $R_{\rm f}$ (0–0) band of $A_2 1 \rightarrow X_2 1$ transition of SbNa.

Moreover, it can be seen from data analysis that the differences between the experimental values and the theoretical ones change from $\left|\nu_{\rm Expt} - \nu_{\rm Cal}\right|_{\rm max}^{J=74} = 0.0043\ {\rm cm}^{-1}$ to $\left|\nu_{\rm Expt} - \nu_{\rm Cal}\right|_{\rm min}^{J=65} = 0.0001\ {\rm cm}^{-1}$ for $R_{\rm e}$-branch, from $\left|\nu_{\rm Expt} - \nu_{\rm Cal}\right|_{\rm max}^{J=25} = 0.0224\ {\rm cm}^{-1}$ to $\left|\nu_{\rm Expt} - \nu_{\rm Cal}\right|_{\rm min}^{J=56} = 0.0001\ {\rm cm}^{-1}$ for $R_{\rm f}$-branch, respectively, which are both illustrated in Fig. 2. Equally important, the estimated error of the unknown experimental data could be predicted from Eq. (8). The maximum values and the minimum values are

$$\left|\Delta\delta\right|_{\rm max}^{J=120} = 0.0390\ {\rm cm}^{-1},\ \ \left|\Delta\delta\right|_{\rm min}^{J=79} = 0\ {\rm cm}^{-1}$$

for $R_{\rm e}$-branch,

$$\left|\Delta\delta\right|_{\rm max}^{J=120} = 0.1390\ {\rm cm}^{-1},\ \ \left|\Delta\delta\right|_{\rm min}^{J=77} = 0.0001\ {\rm cm}^{-1}$$

for $R_{\rm f}$-branch, respectively, which are illustrated in Fig. 5. Comparing Fig. 2 with Fig. 5, we can see from Fig. 6 that the values of deviation $\Delta\delta$ estimated by the unknown experimental data from Eq. (8) almost overlap with the differences in $\nu_{J,{\rm Expt}} - \nu_{J,{\rm DCM}}$, showing the reasonable accuracy of the unknown high-lying transitional emission spectrum. It provides reliable theoretical support for predicting high-lying transitional emission spectral data.

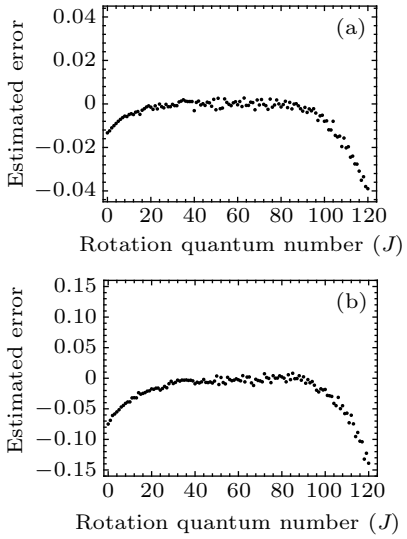


Fig. 5. Estimated error $\Delta\delta$ with rotational quantum numbers J of (a) $R_{\rm e}$ (0–0) band and (b) $R_{\rm f}$ (0–0) band of $A_2 1 \rightarrow X_2 1$ transition of SbNa.

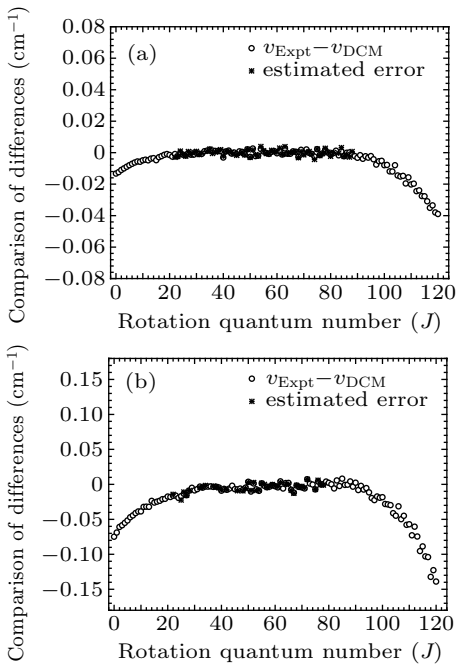


Fig. 6. Estimated error $\Delta\delta$ and difference $(\nu_{J,{\rm Expt}} - \nu_{J,{\rm Cal}})$ transition lines of R-branch transitional emission spectra of (a) $R_{\rm e}$ (0–0) band and (b) $R_{\rm f}$ (0–0) band of $A_2 1 \rightarrow X_2 1$ transition of SbNa.

4. Conclusions

In this work, the DCM method is used to study the R-branch transition emission spectral lines of (0–0) band of the $A_2 1 \rightarrow X_2 1$ transition of SbNa molecule, and only using 11 known experimental transition lines, the high-lying transition spectra up to rotational quantum number $J = 120$ are obtained and analyzed. The calculation results show that the predicted transition lines are consistent with the experimental transition lines. What is more, based on the principle of over determined linear equations, the prediction error $\Delta\delta$ is calculated within an accuracy of 0.01 ${\rm cm}^{-1}$. From all the above we understand that the DCM method to predict unknown transition lines is considered reasonably in this work. These high-lying transition

emission spectral lines provide the valuable reference data for further understanding the internal structure and properties of SbNa molecule. This method also provides a possible way to investigate and analyze a predicted unknown error in diatomic molecule.

Acknowledgement

We thank the Research Center for Advanced Computation of Xihua University for computing support.

Apprendix A: Supporting information

The DCM R-branch transition lines of the (0,0) band of the $A_2 1 \rightarrow X_2 1$ transition of SbNa are listed in Table A1 and Table A2, respectively.

Table A1. Experimental and theoretical R-branch emission spectra and related data of (0,0) band of the $A_2 1 \rightarrow X_2 1$ transition of SbNa (All quantities are in unit cm^{-1}).

J	$R_e(0,0)$ band					
	$v^a_{J,\mathrm{Expt}}$	$v^b_{J,\mathrm{DCM}}$	$v_{J,\mathrm{Expt}} - v_{J,\mathrm{DCM}}$	$\Delta^c_{J,\mathrm{Expt}}$	$\Delta_{J,\mathrm{DCM}}$	$\Delta\delta^d$
		6141.6225				–0.0133
1		6141.8491			0.2265	–0.0124
2		6142.0858			0.2368	–0.0110
3		6142.3328			0.2470	–0.0100
4		6142.5901			0.2572	–0.0090
5		6142.8576			0.2675	–0.0080
6		6143.1353			0.2777	–0.0071
7		6143.4232			0.2879	–0.0063
8		6143.7214			0.2981	–0.0056
9		6144.0307			0.3093	–0.0058
10		6144.3492			0.3185	–0.0049
11		6144.6780			0.3288	–0.0045
12		6145.0169			0.3390	–0.0049
13		6145.3661			0.3492	–0.0038
14		6145.7256			0.3594	–0.0035
15		6146.0963			0.3708	–0.0048
16		6146.4746			0.3782	–0.0029
17		6146.8633			0.3888	–0.0022
18		6147.2628			0.3994	–0.0014
19		6147.6722			0.4094	–0.0009
20		6148.0928			0.4206	–0.0015
21		6148.5241			0.4313	–0.0025
22	**6148.9599**	6148.9628	–0.0029		0.4386	–0.0009
23	6149.4119	6149.4143	–0.0024	0.4520	0.4515	–0.0023
24	6149.8736	6149.8726	0.0010	0.4617	0.4584	–0.0001
25	6150.3426	6150.3438	–0.0012	0.4690	0.4712	–0.0013
26	6150.8232	6150.8254	–0.0022	0.4806	0.4816	–0.0018
27	**6151.3146**	6151.3139	0.0007	0.4914	0.4884	–0.0002
28	6151.8130	6151.8142	–0.0012	0.4984	0.5003	–0.0013
29	6152.3252	6152.3249	0.0003	0.5122	0.5107	–0.0013
30	6152.8446	6152.8438	0.0008	0.5194	0.5190	–0.0002
31	6153.3733	6153.3745	–0.0012	0.5287	0.5306	–0.0008
32	6153.9136	6153.9139	–0.0003	0.5403	0.5395	–0.0008
33		6154.4620			0.5481	0.0009
34	6155.0221	6155.0213	0.0008		0.5593	0.0013
35	6155.5927	6155.5904	0.0023	0.5706	0.5691	0.0019
36	**6156.1693**	6156.1698	–0.0005	0.5766	0.5794	0.0013
37	6156.7597	6156.7593	0.0004	0.5904	0.5896	0.0011
38	6157.3587	6157.3581	0.0006	0.5990	0.5987	0.0011
39	6157.9685	6157.9666	0.0019	0.6098	0.6085	0.0011
40	**6158.5872**	6158.5894	–0.0022	0.6187	0.6228	–0.0031
41	6159.2152	6159.2143	0.0009	0.6280	0.6249	0.0007
42	6159.8522	6159.8514	0.0008	0.6370	0.6371	0.0013
43	6160.5004	6160.5004	0.0000	0.6482	0.6490	–0.0005
44	**6161.1561**	6161.1571	–0.0010	0.6557	0.6567	0.0001
45	6161.8235	6161.8252	–0.0017	0.6674	0.6681	–0.0007
46	6162.5000	6162.5005	–0.0005	0.6765	0.6753	0.0008
47	6163.1870	6163.1867	0.0003	0.6870	0.6861	0.0005
48	6163.8833	6163.8847	–0.0014	0.6963	0.6980	–0.0011
49	6164.5890	6164.5869	0.0021	0.7057	0.7023	0.0021
50	6165.3039	6165.3069	–0.0030	0.7149	0.7200	–0.0027
51	6166.0282	6166.0265	0.0017	0.7243	0.7196	0.0026
52	6166.7641	6166.7654	–0.0013	0.7359	0.7389	–0.0022
53	6167.5070	6167.5091	–0.0021	0.7429	0.7437	–0.0019
54	6168.2616	6168.2577	0.0039	0.7546	0.7486	0.0023
55	**6169.0231**	6169.0219	0.0012	0.7615	0.7642	0.0007
56	6169.7939	6169.7945	–0.0006	0.7708	0.7726	–0.0002
57	6170.5764	6170.5772	–0.0008	0.7825	0.7826	–0.0008
58	6171.3682	6171.3667	0.0015	0.7918	0.7896	0.0005
59	6172.1670	6172.1664	0.0006	0.7988	0.7997	0.0010
60	6172.9775	6172.9771	0.0004	0.8105	0.8107	–0.0004
61	6173.7972	6173.7943	0.0029	0.8197	0.8173	0.0011
62	**6174.6240**	6174.6251	–0.0011	0.8268	0.8308	–0.0012
63	6175.4624	6175.4586	0.0038	0.8384	0.8335	0.0027
64	6176.3077	6176.3085	–0.0008	0.8453	0.8498	–0.0007
65	6177.1647	6177.1647	0.0000	0.8570	0.8562	–0.0007
66	6178.0277	6178.0275	0.0002	0.8630	0.8629	0.0008
67	**6178.9025**	6178.9019	0.0006	0.8748	0.8743	0.0006
68	6179.7857	6179.7889	–0.0032	0.8832	0.8870	–0.0027
69	**6180.6775**	6180.6768	0.0007	0.8918	0.8879	0.0018
70	6181.5794	6181.5808	–0.0014	0.9019	0.9040	–0.0005
71	6182.4889	6182.4886	0.0003	0.9095	0.9078	0.0020
72	6183.4107	6183.4100	0.0007	0.9218	0.9215	–0.0002
73	6184.3380	6184.3389	–0.0009	0.9273	0.9289	–0.0008
74	6185.2738	6185.2781	–0.0043	0.9358	0.9392	–0.0025
75	6186.2219	6186.2196	0.0023	0.9481	0.9415	0.0022
76	6187.1767	6187.1786	–0.0019	0.9548	0.9590	–0.0015
77	6188.1409	6188.1415	–0.0006	0.9642	0.9628	–0.0005
78	6189.1148	6189.1120	0.0028	0.9739	0.9705	0.0018
79	6190.0959	6190.0956	0.0003	0.9811	0.9836	0.0000
80	6191.0851	6191.0874	–0.0023	0.9892	0.9918	–0.0014
81	6192.0853	6192.0852	0.0001	1.0002	0.9978	–0.0003
82		6193.0914			1.0062	0.0012
83	6194.1102	6194.1105	–0.0003		1.0191	–0.0017
84	6195.1364	6195.1332	0.0032	1.0262	1.0227	0.0007
85	**6196.1673**	6196.1697	–0.0024	1.0309	1.0365	–0.0023
86	6197.2086	6197.2098	–0.0012	1.0413	1.0401	–0.0001
87	6198.2572	6198.2600	–0.0028	1.0486	1.0502	0.0001
88	**6199.3208**	6199.3201	0.0007	1.0636	1.0601	–0.0009
89		6200.3888			1.0687	–0.0022
90		6201.4660			1.0772	–0.0033
91		6202.5486			1.0826	–0.0016
92		6203.6434			1.0949	–0.0039
93		6204.7427			1.0992	–0.0023
94		6205.8528			1.1101	–0.0032
95		6206.9693			1.1165	–0.0022
96		6208.0963			1.1271	–0.0042

Table A1. (*Continued*).

J	$R_e(0,0)$ band					
	$\nu^a_{J,\mathrm{Expt}}$	$\nu^b_{J,\mathrm{DCM}}$	$\nu_{J,\mathrm{Expt}}-\nu_{J,\mathrm{DCM}}$	$\Delta^c_{J,\mathrm{Expt}}$	$\Delta_{J,\mathrm{DCM}}$	$\Delta\delta^d$
97		6209.2336			1.1373	–0.0076
98		6210.3732			1.1396	–0.0055
99		6211.5226			1.1494	–0.0052
100		6212.6833			1.1607	–0.0080
101		6213.8488			1.1655	–0.0078
102		6215.0265			1.1778	–0.0119
103		6216.2084			1.1819	–0.0120
104		6217.3936			1.1852	–0.0080
105		6218.5970			1.2034	–0.0145
106		6219.8032			1.2063	–0.0152
107		6221.0151			1.2118	–0.0148
108		6222.2403			1.2253	–0.0196
109		6223.4644			1.2241	–0.0157
110		6224.7045			1.2401	–0.0202
111		6225.9467			1.2422	–0.0197
112		6227.2020			1.2554	–0.0245
113		6228.4596			1.2576	–0.0240
114		6229.7288			1.2692	–0.0276
115		6231.0014			1.2726	–0.0277
116		6232.2847			1.2833	–0.0309
117		6233.5764			1.2917	–0.0351
118		6234.8691			1.2928	–0.0335
119		6236.1752			1.3060	–0.0380
120		6237.4851			1.3099	–0.0390

[a] $\nu_{J,\mathrm{Expt}}$, experimental transition spectra of R-branch from Ref. [17].

[b] $\nu_{J,\mathrm{DCM}}$, calculated transition spectra of R-branch by DCM from Eq. (2) in this work.

[c] Transition spectra difference $\Delta_J = |\nu_{J-1} - \nu_J|$.

[d] $\Delta\delta$, calculated by transition spectra of R-branch from Eq. (8) in this work.

Table A2. Experimental and theoretical R-branch emission spectra and related data of (0,0) band of the $A_2 1 \rightarrow X_2 1$ transition of SbNa (All quantities are in unit cm^{-1}).

J	$R_f(0,0)$ band					
	$\nu^a_{J,\mathrm{Expt}}$	$\nu^b_{J,\mathrm{DCM}}$	$\nu_{J,\mathrm{Expt}}-\nu_{J,\mathrm{DCM}}$	$\Delta^c_{J,\mathrm{Expt}}$	$\Delta_{J,\mathrm{DCM}}$	$\Delta\delta^d$
		6141.6502				–0.0749
1		6141.8750			0.2248	–0.0689
2		6142.1105			0.2355	–0.0609
3		6142.3566			0.2461	–0.0585
4		6142.6134			0.2568	–0.0551
5		6142.8808			0.2674	–0.0516
6		6143.1589			0.2781	–0.0471
7		6143.4475			0.2887	–0.0445
8		6143.7468			0.2993	–0.0411
9		6144.0567			0.3099	–0.0388
10		6144.3773			0.3205	–0.0387
11		6144.7085			0.3312	–0.0322
12		6145.0504			0.3420	–0.0319
13		6145.4033			0.3528	–0.0321
14		6145.7617			0.3584	–0.0237
15		6146.1369			0.3752	–0.0261
16		6146.5213			0.3845	–0.0248
17		6146.9149			0.3935	–0.0235
18		6147.3189			0.4040	–0.0212
19		6147.7336			0.4147	–0.0207
20		6148.1585			0.4249	–0.0175
21		6148.5936			0.4352	–0.0181
22	**6149.0259**	6149.0401	–0.0142		0.4464	–0.0163

Table A2. (*Continued*).

J	$R_f(0,0)$ band					
	$\nu^a_{J,\mathrm{Expt}}$	$\nu^b_{J,\mathrm{DCM}}$	$\nu_{J,\mathrm{Expt}}-\nu_{J,\mathrm{DCM}}$	$\Delta^c_{J,\mathrm{Expt}}$	$\Delta_{J,\mathrm{DCM}}$	$\Delta\delta^d$
23		6149.4957			0.4556	–0.0162
24		6149.9650			0.4693	–0.0194
25	6150.4177	6150.4401	–0.0224		0.4750	–0.0169
26	6150.9153	6150.9262	–0.0109	0.4976	0.4861	–0.0134
27	**6151.4101**	6151.4257	–0.0156	0.4948	0.4995	–0.0156
28	**6151.9176**	6151.9264	–0.0088	0.5075	0.5007	–0.0090
29		6152.4414			0.5150	–0.0050
30		6152.9729			0.5314	–0.0087
31		6153.5094			0.5365	–0.0069
32	6154.0522	6154.0570	–0.0048		0.5476	–0.0032
33	6154.6131	6154.6171	–0.0040	0.5609	0.5601	–0.0047
34	6155.1842	6155.1858	–0.0016	0.5711	0.5686	–0.0031
35		6155.7649			0.5792	–0.0032
36		6156.3544			0.5894	–0.0029
37	6156.9515	6156.9542	–0.0027		0.5999	–0.0036
38	6157.5607	6157.5640	–0.0033	0.6092	0.6098	–0.0033
39	6158.1788	6158.1837	–0.0049	0.6181	0.6197	–0.0044
40	**6158.8074**	6158.8152	–0.0078	0.6286	0.6316	–0.0091
41		6159.4539			0.6386	–0.0065
42	6160.0961	6160.1037	–0.0076	6160.0961	0.6498	–0.0078
43		6160.7619			0.6582	–0.0060
44		6161.4299			0.6679	–0.0020
45		6162.1116			0.6818	–0.0069
46	**6162.7925**	6162.8016	–0.0091		0.6899	–0.0072
47		6163.5009			0.6993	–0.0061
48	6164.2010	6164.2103	–0.0093		0.7094	–0.0079
49	6164.9220	6164.9280	–0.0060	0.7210	0.7177	–0.0047
50	6165.6509	6165.6483	0.0026	0.7289	0.7203	0.0036
51	6166.3890	6166.3978	–0.0088	0.7381	0.7495	–0.0103
52	6167.1391	6167.1365	0.0026	0.7501	0.7386	0.0012
53	6167.8936	6167.9023	–0.0087	0.7545	0.7659	–0.0071
54	6168.6645	6168.6725	–0.0080	0.7709	0.7702	–0.0093
55	6169.4423	6169.4408	0.0015	0.7778	0.7682	0.0014
56	6170.2294	6170.2295	–0.0001	0.7871	0.7887	–0.0021
57	6171.0236	6171.0280	–0.0044	0.7942	0.7985	–0.0041
58	6171.8317	6171.8343	–0.0026	0.8081	0.8063	–0.0032
59	6172.6491	6172.6494	–0.0003	0.8174	0.8152	–0.0010
60	6173.4735	6173.4754	–0.0019	0.8244	0.8260	–0.0027
61	6174.3096	6174.3128	–0.0032	0.8361	0.8374	–0.0043
62	6175.1526	6175.1500	0.0026	0.8430	0.8372	0.0042
63		6176.0129			0.8628	–0.0060
64	6176.8699	6176.8695	0.0004		0.8566	0.0018
65	**6177.7430**	6177.7431	–0.0001	0.8731	0.8736	0.0020
66	6178.6254	6178.6339	–0.0085	0.8824	0.8908	–0.0077
67	**6179.5163**	6179.5290	–0.0127	0.8909	0.8951	–0.0119
68	6180.4191	6180.4205	–0.0014	0.9028	0.8915	–0.0017
69	6181.3303	6181.3342	–0.0039	0.9112	0.9137	–0.0037
70	**6182.2525**	6182.2553	–0.0028	0.9222	0.9210	–0.0044
71	**6183.1794**	6183.1843	–0.0049	0.9269	0.9291	–0.0059
72	6184.1211	6184.1139	0.0072	0.9417	0.9296	0.0073
73		6185.0655			0.9516	0.0011
74		6186.0252			0.9597	–0.0003
75	**6186.9869**	6186.9940	–0.0071		0.9688	–0.0073
76	6187.9663	6187.9603	0.0060	0.9794	0.9663	0.0041
77	6188.9479	6188.9485	–0.0006	0.9816	0.9882	0.0001
78	**6189.9417**	6189.9427	–0.0010	0.9938	0.9942	0.0002
79		6190.9397			0.9970	0.0039
80		6191.9521			1.0124	0.0021
81		6192.9744			1.0223	0.0001

Table A2. (*Continued*).

J	$R_f(0,0)$ band					
	$v^a_{J,\mathrm{Expt}}$	$v^b_{J,\mathrm{DCM}}$	$v_{J,\mathrm{Expt}} - v_{J,\mathrm{DCM}}$	$\Delta^c_{J,\mathrm{Expt}}$	$\Delta_{J,\mathrm{DCM}}$	$\Delta\delta^d$
82		6194.0094			1.0350	–0.0059
83		6195.0385			1.0290	0.0056
84		6196.0916			1.0531	–0.0024
85		6197.1390			1.0474	0.0081
86		6198.2096			1.0706	–0.0008
87		6199.2840			1.0743	–0.0005
88		6200.3626			1.0786	0.0041
89		6201.4583			1.0958	–0.0033
90		6202.5526			1.0943	0.0023
91		6203.6688			1.1162	–0.0082
92		6204.7786			1.1098	–0.0022
93		6205.9106			1.1320	–0.0075
94		6207.0411			1.1305	–0.0054
95		6208.1891			1.1480	–0.0115
96		6209.3456			1.1565	–0.0196
97		6210.5032			1.1576	–0.0225
98		6211.6665			1.1633	–0.0174
99		6212.8423			1.1758	–0.0192
100		6214.0267			1.1844	–0.0184
101		6215.2246			1.1979	–0.0281
102		6216.4270			1.2024	–0.0287
103		6217.6341			1.2071	–0.0297
104		6218.8612			1.2271	–0.0412
105		6220.0858			1.2246	–0.0449
106		6221.3092			1.2234	–0.0314
107		6222.5611			1.2519	–0.0498
108		6223.8049			1.2438	–0.0450
109		6225.0740			1.2691	–0.0579
110		6226.3338			1.2597	–0.0571
111		6227.6179			1.2841	–0.0729
112		6228.8923			1.2744	–0.0605
113		6230.1854			1.2931	–0.0746
114		6231.4876			1.3022	–0.0954
115		6232.7950			1.3074	–0.0887
116		6234.1142			1.3192	–0.1030
117		6235.4312			1.3170	–0.1040
118		6236.7661			1.3349	–0.1323
119		6238.1080			1.3419	–0.1227
120		6239.4497			1.3417	–0.1390

References

[1] Anderson C G 2012 *Geochemistry* **72** 3

[2] Qu H Q, Wu W H, Zheng Y J, Xie J X and Xu J Z 2011 *Fire Safety Journal* **46** 462

[3] Shura M W 2020 *Physica B* **580** 411942

[4] Nakayama M, Fujita H, Morohara O, Geka H, Sakurai Y, Yasuda D, Suzuki M, Shibata Y and Kuze N 2020 *Phys. Status Solidi A* **217** 1900515

[5] Ning X M, Zhou X S, Luo J, Ma L and Zhan L 2019 *Nanotechnology* **31** 095404

[6] He J, Wei Y Q, Zhai T Y and Li H Q 2018 *Mater. Chem. Front.* **2** 437

[7] Liu Z M, Song T and Paik U 2018 *J. Mater. Chem. A* **6** 8159

[8] An Y B, Xu X Y, Sun Q X, Cao X B, Wen W L, Wang J F, Liu H L, Lu Y, Tian J S, Li X F and Li Y H 2014 *Acta Opt. Sin.* **34** 333

[9] Fan Q C, Hu C P, Fu J, Ma J, Fan Z X, Xu Y G, Li H D and Zhang Y 2018 *Spectrochim Acta A* **200** 290

[10] Zhang Y P, Deng L H, Zhang J and Chen Y Q 2015 *Chin. J. Chem. Phys.* **28** 134

[11] Lang F, Winkler K, Strauss C, Grimm R and Denschlag J H 2008 *Phys. Rev. Lett.* **101** 133005

[12] Evans H E and Watson W R 1971 *J. Nucl. Mater.* **40** 195

[13] Redslob H, Steinleitner G and Freyland W 1982 *Zeitschrift für Naturforschung A* **37** 587

[14] Dolizy P and Groliere F 1986 *J. Phys. D: Appl. Phys.* **19** 687

[15] Songster J and Pelton A D 1993 *J. Phase Equilib.* **14** 250

[16] Liu Y J, Xu J, Kang Z T and Wang J 2013 *Thermochim Acta* **569** 119

[17] Setzer K D, Fink E H, Liebermann H P, Buenker R J and Alekseyev A B 2015 *J. Mol. Spectrosc.* **318** 1

[18] Phoebe K A, John M G, Ali D, Olaf J B, Kamila M W, Karena W C, Andrew J M, Peter J C, Laure M and Clare P G 2016 *J. Am. Chem. Soc.* **138** 2352

[19] Wang N, Wan M J, Zhang C Z, Jin Y Y, Zhang W B, Chen S J and Li S 2019 *Spectrochim Acta A* **208** 124

[20] Wang N, Lu N, Zhang W B, Zhang C Z, Jin Y Y, Wan M J and Li S 2020 *Spectrochim Acta A* **224** 117413

[21] Tennyson J, Lodi L, Mckemmish L K and Yurchenko S N 2016 *J. Phys. B-At. Mol. Opt.* **49** 102001

[22] Fu J, Long S S, Jian J, Fan Z X and Ma J 2020 *Spectrochim Acta A* **239** 118363

[23] Fan Z X, Sun W G, Zhang Y, Fu J, Hu S D and Fan Q C 2018 *Phys. Plasmas* **25** 033301

[24] Zhang L L, Sun W G, Zhang Y, Fan Z X, Hu S D and Fan Q C 2017 *J. Phys. B* **50** 085201

[25] Sun W G, Fan Q C, Li H D and Feng H 2011 *Spectrochim Acta A* **79** 35

[26] Jiang Y H, Sun W G, Zhang Y, Fu J, Fan Q C, Li H D and Feng H 2016 *Spectrochim Acta A* **153** 87

[27] Herzberg G and Mrozowski S 1950 *Molecular Spectra and Molecular Structure. I. Spectra of Diatomic Molecules* (New York: Nostrand D Van Printing)